ORIGINAL ARTICLE

Journal of Cachexia, Sarcopenia and Muscle 2022; **13**: 467–480
Published online 8 December 2021 in Wiley Online Library (wileyonlinelibrary.com) **DOI:** 10.1002/jcsm.12841

Systemic ablation of vitamin D receptor leads to skeletal muscle glycogen storage disorder in mice

Anamica Das[1], Suchitra D. Gopinath[2*] & Gopalakrishnan Aneeshkumar Arimbasseri[1*]

[1]*Molecular Genetics Laboratory, National Institute of Immunology, New Delhi, India,* [2]*Translational Health Science and Technology Institute, Faridabad, Haryana, India*

Abstract

Background Vitamin D deficiency leads to pathologies of multiple organ systems including skeletal muscle. Patients with severe vitamin D deficiency exhibit muscle weakness and are susceptible to frequent falls. Mice lacking a functional vitamin D receptor (VDR) develop severe skeletal muscle atrophy immediately after weaning. But the root cause of myopathies when vitamin D signalling is impaired is unknown. Because vitamin D deficiency leads to metabolic changes as well, we hypothesized that the skeletal muscle atrophy in mice lacking VDR may have a metabolic origin.

Methods We analysed wild-type (WT) mice as well as vitamin D receptor null (vdr−/−) mice for skeletal muscle proteostasis, energy metabolism, systemic glucose homeostasis, and muscle glycogen levels. Dysregulation of signalling pathways as well as the glycogen synthesis and utilization machinery were also analysed using western blots. qRT–PCR assays were performed to understand changes in mRNA levels.

Results Skeletal muscles of vdr−/− exhibited higher expression levels of muscle-specific E3 ubiquitin ligases and showed increased protein ubiquitination, suggesting up-regulation of protein degradation. Foxo1 transcription factor was activated in vdr−/− while Foxo3 factor was unaffected. Fasting protein synthesis as well as mTORC1 pathways were severely down-regulated in vdr−/− mice. Skeletal muscle ATP levels were low in vdr−/− (0.58 ± 0.18 μmol/mL vs. 1.6 ± 0.0.14 μmol/mL, $P = 0.006$), leading to increased AMPK activity. Muscle energy deprivation was not caused by decreased mitochondrial activity as we found the respiratory complex II activity in vdr−/− muscles to be higher compared with WT (0.29 ± 0.007 mU/μL vs. 0.16 ± 0.005 mU/μL). vdr−/− mice had lower fasting blood glucose levels (95 ± 14.5 mg/dL vs. 148.6 ± 6.1 mg/dL, $P = 0.0017$) while they exhibited hyperlactataemia (7.42 ± 0.31 nmol/μL vs. 4.95 ± 0.44 nmol/μL, $P = 0.0032$), suggesting systemic energy deficiency in these mice. Insulin levels in these mice were significantly lower in response to intraperitoneal glucose injection (0.69 ± 0.08 pg/mL vs. 1.11 ± 0.09 pg/mL, $P = 0.024$). Skeletal muscles of these mice exhibit glycogen storage disorder characterized by increased glycogen accumulation. The glycogen storage disorder in vdr−/− muscles is driven by increased glycogen synthase activity and decreased glycogen phosphorylase activity. Increased glycogenin expression supports higher levels of glycogen synthesis in these muscles.

Conclusions The results presented show that lack of vitamin D signalling leads to a glycogen storage defect in the skeletal muscles, which leads to muscle energy deprivation. The inability of vdr−/− skeletal muscles to use glycogen leads to systemic defects in glucose homeostasis, which in turn leads to proteostasis defects in skeletal muscles and atrophy.

Keywords Vitamin D; VDR; Glycogen; Skeletal muscle; Atrophy; Proteostasis; Energy metabolism; Glucose homeostasis

Received: 20 April 2021; Revised: 31 August 2021; Accepted: 27 September 2021
**Correspondence to: Gopalakrishnan Aneeshkumar Arimbasseri, Molecular Genetics Laboratory, National Institute of Immunology, Aruna Asaf Ali Marg, New Delhi 110067, India. Email: aneesh@nii.ac.in; Suchitra D. Gopinath, Translational Health Science and Technology Institute, Faridabad, Haryana 121001, India. Email: sgopinath@thsti.res.in*

Introduction

Apart from severe bone mineralization defects, alopecia, and other metabolic defects, vitamin D receptor knockout (vdr−/−) mice develop severe skeletal muscle atrophy.[1] Vitamin D deficiency induces myopathy in humans as well as experimental animals,[2] and vitamin D receptor (VDR) is shown to be expressed in skeletal muscles, albeit at low levels.[3,4] But the aetiology of skeletal muscle atrophy in the absence of VDR signalling is unknown. Several studies have shown that vitamin D signalling defects lead to metabolic impairments including insulin resistance. But the role of metabolic derangement in the origin of myopathies in the absence of vitamin D signalling is unexplored.

Protein homeostasis is the major determinant of skeletal muscle mass.[5] Muscle protein synthesis increases in response to nutrients and growth factors while during the post-absorptive state, muscle catabolizes proteins and releases amino acids to the bloodstream.[6] Muscle protein homeostasis is important for maintenance of organismal energy homeostasis. Skeletal muscles function as a major site of glucose disposal and fatty acid utilization. Furthermore, energy deprivation conditions lead to increased muscle proteolysis so that the amino acids released can be used for gluconeogenesis,[7,8] thus linking systemic energy metabolism to muscle mass. Conversely, changes in skeletal muscle metabolism affect the systemic energy metabolism as evidenced by the rewiring of whole body glucose metabolism upon disinhibition of muscle fatty acid oxidation.[9]

Multiple factors can induce an imbalance in these activities, often leading to skeletal muscle atrophy. For example, when the demand for amino acids is increased under conditions such as sepsis and burns, muscle protein degradation and amino acid release are up-regulated substantially, leading to skeletal muscle atrophy.[10,11] Alternatively, energy deprivation conditions such as starvation, cachexia, and type I diabetes also lead to skeletal muscle atrophy.[7,8] Here, we explored the role of metabolic impairments in the development of skeletal muscle atrophy in vdr−/− mice.

Some evidence from vitamin D-deficient rat models had shown increased proteolysis in skeletal muscles.[12] Moreover, mTOR activity, which plays an important role in the skeletal muscle mass, is also reduced in this model,[13] clearly suggesting the role of vitamin D signalling in maintaining protein homeostasis in skeletal muscles. But the molecular and metabolic defects that drive these changes in the absence of vitamin D signalling are unknown. Even though myocyte-specific VDR knockout mice exhibited sarcopenia suggesting that muscle intrinsic VDR signalling is important for maintenance of muscle strength and function during ageing,[14] these mice as well as skeletal muscle-specific VDR knockout mice did not display the severe skeletal muscle pathogenesis observed in whole body VDR knockout, suggesting a role for systemic or local modulators in the onset of atrophy in vdr−/− mice.[14,15]

In this study, we attempted the root cause analysis of skeletal muscle atrophy in vdr−/− mice. Indeed, this genetic model of vitamin D deficiency also exhibits dysregulation of muscle proteostasis characterized by increased proteolysis, decreased mTORC1 activity, and fasting protein synthesis. These proteostasis defects are associated with a systemic energy deprivation indicated by hypoglycaemia and hyperlactataemia. As a result, AMPK pathway and Foxo1 transcription factor were activated in skeletal muscles, leading to up-regulation of the atrophy markers. Further attempts to identify the cause for the energy deficiency and atrophy revealed dysregulation of glycogen synthase and glycogen phosphorylase activities resulting in increased glycogen storage levels in the skeletal muscles. Data presented here show that defective muscle and systemic energy metabolism defects caused by glycogen storage disorder in skeletal muscles drive severe muscle atrophy in vdr−/− mice.

Methods

Animal maintenance

Vitamin D receptor null mutant mice were obtained from Jackson Laboratories (Stock No. 006133, B6.129S4-Vdrtm1Mbd lJ; Bar Harbor, ME, USA) and bred at the Small Animal Facility at the National Institute of Immunology, New Delhi, India. Heterozygous mating pairs were set up, and genotyping was done for each litter. vdr−/− and vdr +/+ from the same litter were used as experimental and control groups. All mice were fed ad libitum with a commercially available rodent chow (Altromin International). Both male and female mice were used for the study as there was no difference in the parameters checked. Experiments were performed on mice at 3, 5, or 7 weeks of age as indicated in the text. Mice were housed in a sterile facility in individually ventilated cages (IVC).

RNA extraction and quantitative RT–PCR

Quad muscles were dissected and snap-frozen in liquid nitrogen and homogenized in RNAiso plus Reagent (TAKARA, 1 mL/100 mg tissue) to isolate total muscle RNA as per the manufacturer's recommendations. Total RNA was quantified with a Nanodrop 8000 Spectrophotometer (Thermo Scientific, Wilmington), and a ratio of 2 for the absorbance of 260 to 280 nm was used to determine the RNA quality. First-strand cDNA was synthesized from total RNA using the PrimeScript First-Strand cDNA Synthesis Kit with PrimeScript Reverse Transcriptase according to the manufacturer's protocols (TAKARA). Quantitative RT–PCR was performed using the

QuantStudio-6 and -7 Flex Real-Time PCR Systems (Thermo Fisher Scientific) with *SYBR® Premix Ex Taq* (Tli RNase H Plus) by TAKARA. Each sample was amplified in triplicates using primers specific to Murf1, Fbxo32, GBE1, glycogenin, Glut1, Glut4, UCP2, UCP3, and glyceraldehyde 3-phosphate dehydrogenase (GAPDH). The expression levels of each transcript were normalized to the housekeeping gene GAPDH. The primer sequences used are available upon request.

Western blotting and antibodies

Protein extracts from the hindlimb muscles of wild-type (WT) and VDR−/− mice were obtained by homogenizing muscles in lysis buffer (50 mM Tris–HCl pH 7.5, 150 mM NaCl, 5 mM EDTA, 1% NP-40, 0.5% sodium deoxycholate, 0.1% SDS) containing protease/phosphatase inhibitor cocktail (Cell Signaling Technology). The proteins were resolved by SDS-PAGE (8%, 10%, 12%, and 15%) and transferred onto nitrocellulose membrane (BioRad and Himedia). The membranes were incubated with primary antibodies followed by incubation with HRP-conjugated anti-mouse or anti-rabbit secondary antibodies and visualized using Supersignal West Pico Chemiluminescent Substrate (Thermo Scientific, Rockford, IL, USA). Blots were probed with antibodies against the gene of interest.

Glucose tolerance and serum insulin estimation

To examine alterations in glucose tolerance and insulin secretion, WT and homozygous VDR mutant mice were deprived of food in their normal cage environment for a period of 7 h. During that period, the mice had free access to water. Glucose (2 mg/kg body weight) was administered at time 0 by intravenous injection in saline. Blood glucose levels at 0, 10, 30, 60, and 120 min were determined in whole blood from the tip of the tail using the Accu-Chek Active Glucometer. Serum samples for measurement of insulin levels were obtained from the retro orbital venous plexus at baseline and 30 min after an intraperitoneal glucose challenge.

In vivo estimation of muscle protein synthesis

For SUnSET assay, mice were fasted for 7 h and then given an intraperitoneal injection of 0.040 μmol/g puromycin dissolved in 100 μL of PBS. At exactly 30 min after injection, tibialis anterior (TA) muscle was collected and frozen in liquid N_2 for western blot analysis as described in a previous section. A mouse IgG2a monoclonal anti-puromycin antibody (clone 12D10, 1:5000) was used to detect puromycin incorporation. To check the postprandial protein synthesis, 200 μL of food dissolved in water was given via oral gavage. Puromycin was injected 30 min after feeding, and TA muscle was harvested 30 min post-puromycin injection.

In vivo estimation of protein ubiquitination

Mice at 7 weeks were injected intraperitoneally with a proteasomal inhibitor, MG132 (2.5 mg/kg/day in 20% DMSO daily) for 2 days. Mice were euthanized, hindlimb muscles were harvested and lysed, and western blot analysis was performed as described in a previous section. To detect total protein ubiquitination, anti-ubiquitin antibody (Cloud-Clone Corp.) was used. To detect the K48-linked ubiquitination, anti-K48 ubiquitin antibody (Cell Signaling Technology) was used.

ATP estimation in muscles

ATP estimation was done using the kit from Thermo Scientific. A total of 100 mg of tissue was chopped using a scalpel into small pieces and sonicated in a modified RIPA buffer with EDTA (150 mM NaCl, 1% NP40, 0.5% Na-deoxycholate, 0.1% SDS, 25 mM Tris, pH 7.4) and centrifuged at maximum speed for 15 min at 4°C. The supernatant was collected and proceeded with the assay according to the manufacturer's protocol.

Histological analyses

Skeletal muscle tissue (TA) for histology was collected from 7-week-old WT and frozen in isopentane chilled in liquid nitrogen. Ten-micrometre sections were cut using a cryotome (Thermo Scientific). These sections were stained with periodic acid-Schiff (PAS) according to the manufacturer's protocol (Sigma). The muscle sections were blindly analysed by a pathologist, and the pics were taken at ×400 magnification (scale bar = 20 μm). For succinate dehydrogenase (SDH) staining of muscle sections, frozen sections of skeletal muscles were incubated for 50 min in a humidified chamber at 37°C with incubation media [100 mM phosphate buffer, pH 7.6, 1.2 mM nitroblue tetrazolium (NBT), and 100 mM sodium succinate] followed by imaging.

Serum calcium, lactate, growth hormone, and insulin-like growth factor 1 estimation

Serum lactate was estimated using lactate estimation kit (Abcam #ab65331) and calcium estimation kit (Abcam #ab102505) according to the manufacturer's instructions. Growth hormone (GH) and Igf1 were estimated using ELISA kits as per the manufacturer's protocols (Krishgen Biosystems, Mumbai, India).

Muscle succinate dehydrogenase and pyruvate dehydrogenase estimations

Assays were done from muscle lysates prepared in the assay buffer as per the manufacturer's protocol (Sigma-Aldrich).

Statistics

Densitometric quantification of western blots was performed using ImageJ software. All experiments were repeated at least three times. Number for samples per each figure is indicated as data points in the figure. For western and real-time PCR quantifications, pairwise comparisons were made using parametric, unpaired *T*-test with unequal variance. For all other experiments, a parametric, paired *T*-test with equal variance was used. *F* test was performed to determine if samples had equal variance or unequal variance. Graphs show the mean of the indicated number of replicates, and error bars represent standard error of the mean (SEM). All graphs were prepared using GraphPad Prism software Version 9.

Results

vdr−/− mice exhibit higher muscle protein degradation

As reported previously,[1,16] body weights of the vdr−/− mice were comparable with that of WT littermates in the pre-weaning stage, whereas in the post-weaning stage, they exhibited progressive growth retardation as indicated by reduced body weight at 5 and 7 weeks of age (Supporting Information, *Figure* S1a). These mice exhibit a high rate of mortality beyond 8 weeks of age.[17] Additionally, vdr−/− mice also exhibited reduced weights of TA, gastrocnemius (GAS), and quadriceps (QUAD) muscles at 7 weeks of age (*Figure* S1b–S1d) as documented in previous studies.[1] Histopathology analysis of cross sections of TA and GAS muscles also shows reduced fibre size in these muscles (*Figure* S1e–S1g).

Next, we asked if the reduced muscle mass in vdr−/− is indicative of active muscle wasting or the failure of these mice to grow. Because the GH–insulin-like growth factor (IGF) 1 axis controls the growth as well as muscle mass in mammals,[10,18] we checked their levels in the sera of these mice and found reduced GH levels (*Figure*). Because GH release by pituitary is pulsatile, there can be temporal variations in its levels. So, we checked the levels of IGF1 as it is induced by GH, more stable in serum, and acts as the major downstream effector of GH.[19] Intriguingly, IGF1 levels were unchanged in the serum of these mice (*Figure* 1B), suggesting that the GH–IGF1 axis may not be drastically affected in these mice. Irrespective of the inducing factor, severe muscle atrophy is almost always associated with increased protein degradation and the up-regulation of muscle-specific E3 ubiquitin ligases.[20] We analysed protein ubiquitination levels in both 3- (no atrophy) and 7-week-old (severe atrophy) WT and vdr −/− mice as a proxy for proteasomal degradation. After 2 days of intraperitoneal injection with the proteasome inhibitor MG132, both total ubiquitination and K48-linked ubiquitination, which is specific to proteasomal degradation pathway, were high in 7-week-old vdr−/− skeletal muscle (*Figure* 1C). Two major muscle-specific E3 ubiquitin ligases Fbxo32 and MuRF1 are well-known atrophy markers and are up-regulated in the majority of skeletal muscle atrophies.[21] Indeed, the mRNA levels of both Fbxo32 and MuRF1 were up-regulated in the 7-week-old vdr−/− compared with WT (*Figure* 1D and 1E), highlighting that the up-regulation of proteasomal protein degradation is associated with the muscle atrophy in these mice.

FoxO proteins are the key transcription factors that drive muscle atrophy in response to a variety of stimuli. Furthermore, overexpression of Foxo3 and Foxo1 induces atrophy in skeletal muscles.[22] Intriguingly, neither the total protein levels nor the nucleo-cytoplasmic localization of Foxo3 protein were altered in vdr−/− compared with WT (*Figure* S2a–S2c). On the other hand, as observed previously,[15] Foxo1 protein levels were significantly increased in the 7-week-old vdr−/− muscles (*Figure* 1F). The ratio of Foxo1 phosphorylated at Ser256, which is the inactive cytoplasmic form, to the total Foxo1 was dramatically reduced in these mice (*Figure* 1G and 1H), suggesting that abnormal activation of Foxo1 is responsible for the increased transcript levels of Fbxo32 and MuRF1 as well as the increased protein ubiquitination levels. In support of this, the nuclear localization of Foxo1 was also higher in vdr−/− skeletal muscles (*Figure* 1I).

mTORC1 pathway and fasting protein synthesis are down-regulated in the skeletal muscles of vdr−/− mice

Apart from the increased proteasomal protein degradation, defective regulation of protein synthesis is also associated with several skeletal muscle atrophy models.[18,23] Muscle protein synthesis is up-regulated by amino acids as well as insulin during the absorptive state. On the other hand, during the post-absorptive state, only basal rates of protein synthesis are maintained.[6] To address if there are defects in protein synthesis in absorptive and fasting states in the skeletal muscles of vdr−/− mice, we performed *in vivo* SUnSET assay. WT and vdr−/− mice were either fasted for 7 h (fasting protein synthesis) or fed a liquid diet after fasting by oral gavage (absorptive state protein synthesis) followed by an intraperitoneal injection of puromycin. Western blot analysis of

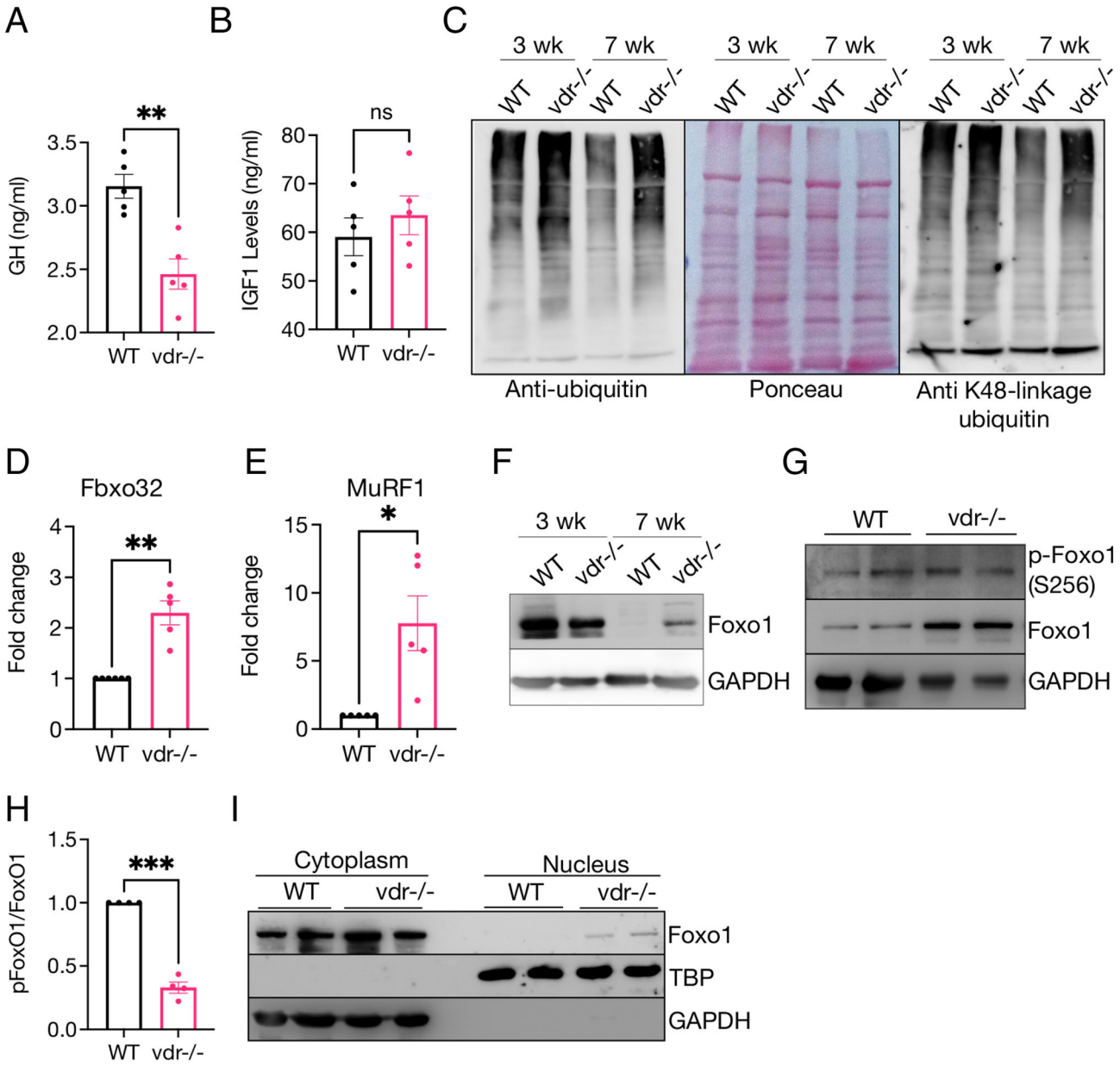

Figure 1 vdr−/− mice exhibit higher muscle protein degradation. *(A* and *B)* Serum levels of growth hormone *(A)* and IGF1 *(B)* measured using ELISA. *(C)* Anti-ubiquitin and anti-ubiquitin–K48-linkage western blots of hindlimb skeletal muscle extracts of mice treated with proteasome inhibitor MG132. Ponceau staining of the blot is shown for equal loading. *(D* and *E)* Expression levels of Fbxo32 *(D)* and MuRF1 *(E)* mRNAs in hindlimb muscles of 7-week-old WT and vdr−/− quantified using qRT–PCR ($n \geq 4$). *(F)* Representative western blot for Foxo1 protein levels in hindlimb skeletal muscles of 3- and 7-week-old WT and vdr−/− mice. *(G* and *H)* Western blot showing the levels of phospho-Foxo1 (Ser256) *(G)* and the ratio of phospho-Foxo1 to total Foxo1 *(H)*. *(I)* Western blot analysis showing nuclear localization of Foxo1 in WT and vdr−/− mice. Anti-TBP antibody was used as a nuclear marker, and anti-GAPDH was used as a cytoplasmic marker. All graphs show mean ± SEM. Statistical significance was determined by unpaired *T*-test (*: $P < 0.05$, **: $P < 0.01$, ***: $P < 0.001$, ****: $P < 0.0001$).

hindlimb skeletal muscles harvested 30 min after puromycin injection showed similar levels of puromycin incorporation in 3-week-old WT and vdr−/− fasted mice (*Figure* 2A). On the contrary, 7-week-old vdr−/− mice exhibited a drastic decrease in fasting protein synthesis compared with their WT counterparts (*Figure* 2B). Interestingly, there was no difference in the rates of absorptive state protein synthesis in the muscles of 7-week-old WT and vdr−/− mice (*Figure* 2C). These results show that muscle atrophy in vdr−/− mice is associated with a proteostasis defect characterized by a general increase in protein degradation and a decrease in post-absorptive protein synthesis.

To investigate the molecular mechanisms underlying altered protein synthesis, we examined the mammalian target

DOI: 10.1002/jcsm.12841

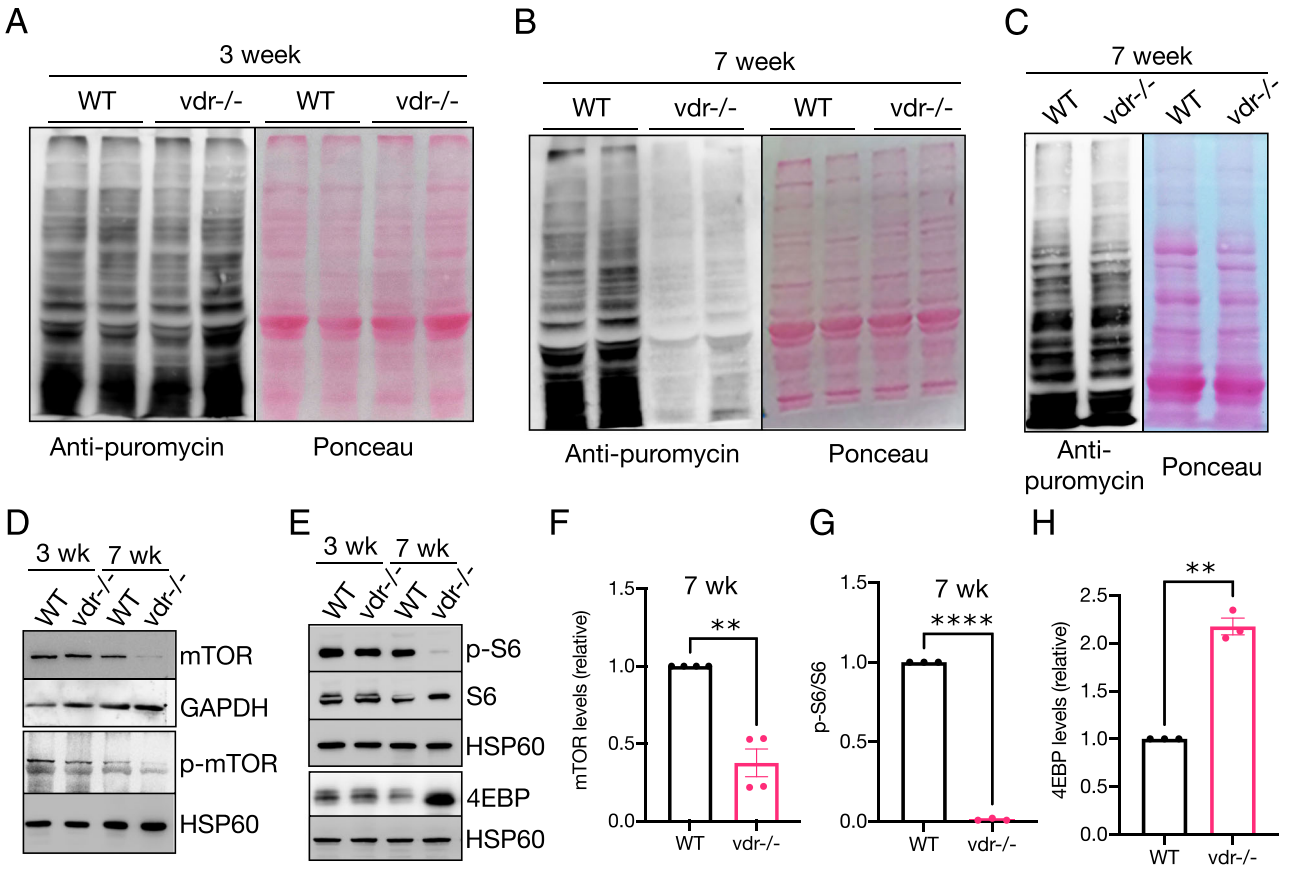

Figure 2 mTORC1 pathway and fasting protein synthesis are down-regulated in the skeletal muscles of vdr−/− mice. *(A–C)* Western blots using anti-puromycin antibody for estimation fasting protein synthesis in 3-week-old *(A)* and 7-week-old *(B)* and absorptive state protein synthesis in 7-week-old *(C)* hindlimb muscles of WT and vdr−/−. Image of a Ponceau stained blot is used as loading control. *(D)* Western blots for phospho and total mTORC1 protein in 3- and 7-week-old mice. *(E)* Western blots for S6 and 4EBP levels in 3- and 7-week-old mice. *(F–H)* Quantitation of mTOR protein *(F)*, phospho-S6 *(G)*, and 4EPB *(H)* bands from *(D)* and *(E)*. All graphs show mean ± SEM. Statistical significance was determined by unpaired *T*-test (*: $P < 0.05$, **: $P < 0.01$, ***: $P < 0.001$, ****: $P < 0.0001$).

of Rapamycin Complex 1 (mTORC1) signalling pathway, which acts as the central regulator of cell growth partly by increasing protein synthesis.[24] Recent studies have shown evidence for dysregulation of mTORC1 in a vitamin D-deficient rat model system.[12,13] When compared with WT, mTOR protein levels were unchanged in 3-week-old vdr−/− mice (*Figure* 2D). On the other hand, 7-week-old vdr−/− mice exhibited significantly lower levels of mTOR protein, suggesting that skeletal muscle atrophy is associated with down-regulation of mTORC1 pathway (*Figure* 2D and 2F). Concomitantly, levels of mTOR phosphorylated at Ser2448 and ribosomal protein S6 phosphorylated at Ser240/244, both performed by the mTORC1 target p70-S6K, were reduced in 7-week-old vdr−/− muscles, confirming the down-regulation of the mTORC1 pathway (*Figure* 2E and 2G). Additionally, western blot analysis of 4EBP1, a repressor of cap-dependent translation and an mTORC1 target,[25] displayed increased protein levels in 7-week-old vdr−/− muscles, with the majority of protein belonging to the fast migrating, hypo-phosphorylated band (*Figure* 2E and 2H), further confirming reduced mTORC1 activity. Taken together, our observations strongly indicate that reduced protein synthesis driven by defective mTORC1 activity and increased protein degradation induced by Foxo1 activation could be driving skeletal muscle atrophy in vdr−/− mice.

vdr−/− skeletal muscles exhibit energy deprivation

Next, we asked what is the root cause of the defective proteostasis in vdr−/− mice. Various triggers ranging from inflammation to metabolic disorders and energy deprivation can affect skeletal muscle proteostasis and mTORC1 activity. Insulin signalling as well as growth factor signalling represses Foxo1 and activates mTORC1 activity while energy deprivation conditions such as starvation do the opposite.[26] Interestingly, we observed an up-regulation of insulin receptor (IR) expression in the vdr−/− skeletal muscles compared with WT muscles (*Figure* 3A). However, phosphorylation of IR at

DOI: 10.1002/jcsm.12841

Tyr1345, which is induced by activation of IR, was reduced, suggesting lower IR pathway activity (*Figure* 3B and 3C). Moreover, the levels of the adapter protein IRS1 were significantly low in vdr−/− muscles, strongly indicating reduced insulin signalling (*Figure* 3B). The activating Ser473 phosphorylation of AKT/PKB, an effector of the IR pathway and an activator of mTORC1 complex, was also reduced in vdr−/− muscles compared with WT (*Figure* 3D and 3E). In agreement with this, similar to the mice with mutations in the VDR DNA binding domain,[27] 7-week-old vdr−/− mice displayed defective insulin response following intraperitoneal glucose injection (*Figure* 3F). So, it is likely that the increased IR protein levels could be a compensatory mechanism to counteract the absence of insulin response, but this increase could not restore the IR pathway.

Conditions that lead to energy deprivation activate AMPK pathway and increase IR expression levels,[28] and it is well established that the AMPK pathway inhibits the mTORC1

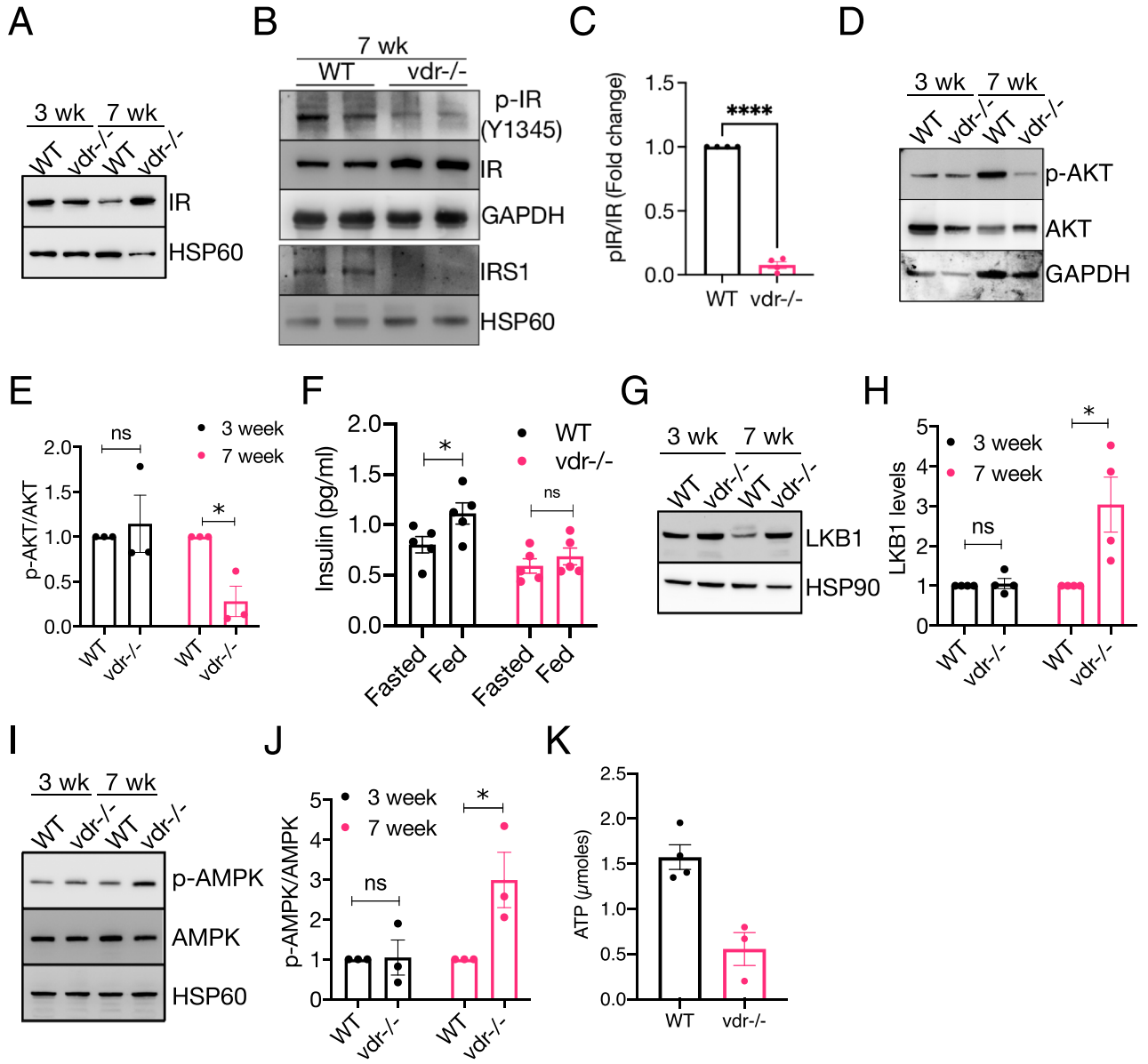

Figure 3 vdr−/− skeletal muscles exhibit energy deprivation. *(A)* Representative western blot for insulin receptor in 3- and 7-week-old WT and vdr−/−. *(B)* Western blots for phospho-IR (Tyr1345), IR, and IRS1. *(C)* Ratio of phospho-IR to total IR (n = 4). *(D and E)* Western blot for p-AKT in 3- and 7-week-old WT and vdr−/− *(D)* and quantitation of bands *(E)* (n = 3). *(F)* Serum insulin levels measured by ELISA at fasting state and 10 min after intraperitoneal injection of glucose (n = 5). *(G–J)* Representative western blots for LKB1 and AMPK *(G, I)* and their densitometric quantification *(H, J)* (n = 3). *(K)* Muscle ATP levels in WT and vdr−/−. All graphs show mean ± SEM. Statistical significance was determined by unpaired T-test (*: $P < 0.05$, **: $P < 0.01$, ***: $P < 0.001$, ****: $P < 0.0001$).

DOI: 10.1002/jcsm.12841

pathway.[29,30] Accordingly, protein levels of LKB1, the upstream activator of AMPK pathway, were significantly higher in the skeletal muscles of vdr−/− mice compared with WT (*Figure* 3G and 3H). Although total AMPK protein levels did not show any difference, there was a sharp increase in the levels of Thr172 phosphorylated AMPK in vdr−/− muscles (*Figure* 3I and 3J), indicating activation of the AMPK pathway. Indeed, ATP levels were significantly lower in vdr−/− muscles than WT, clearly indicating energy deprivation (0.58 ± 0.18 μmol/mL vs. 1.6 ± 0.0.14 μmol/mL, $P = 0.006$) (*Figure* 3K). Consistent with a systemic metabolic imbalance, we observed lower p-S6 levels in vdr−/− livers, indicative of reduced mTORC1 activity (*Figure* S3a). However, AMPK activity in the vdr−/− liver was comparable with that of WT (*Figure* S3b). Additionally, 7-week-old vdr−/− mice did not exhibit any difference in liver fasting protein synthesis, suggesting that protein synthesis in skeletal muscles is more susceptible to energy imbalances in the vdr−/− mice (*Figure* S3c).

Energy insufficiency in vdr−/− skeletal muscles is not due to diminished mitochondrial activity.

Decreased ATP levels in vdr−/− skeletal muscles may indicate defective mitochondrial biogenesis. On the other hand, energy deficiency conditions that lead to activation of the AMPK pathway are well established to increase mitochondrial biogenesis to meet the energy demands.[31] To understand the underlying reason for the energy deprivation in vdr−/− skeletal muscles, it is essential to delineate these two scenarios. We postulated that if the energy deprivation is due to mitochondrial biogenesis defect, there should be a decrease in mitochondrial protein content. To address this, we performed western blot analysis of different classes of mitochondrial proteins in WT and vdr−/− mice. TOMM20, a central component of the mitochondrial protein import machinery located on the outer membrane, was unchanged in the vdr−/− mice (*Figures* 4A and S4a). TOMM20 is considered as a marker for mitochondrial mass,[32] and this datum indicates that despite having lower energy levels, vdr−/−

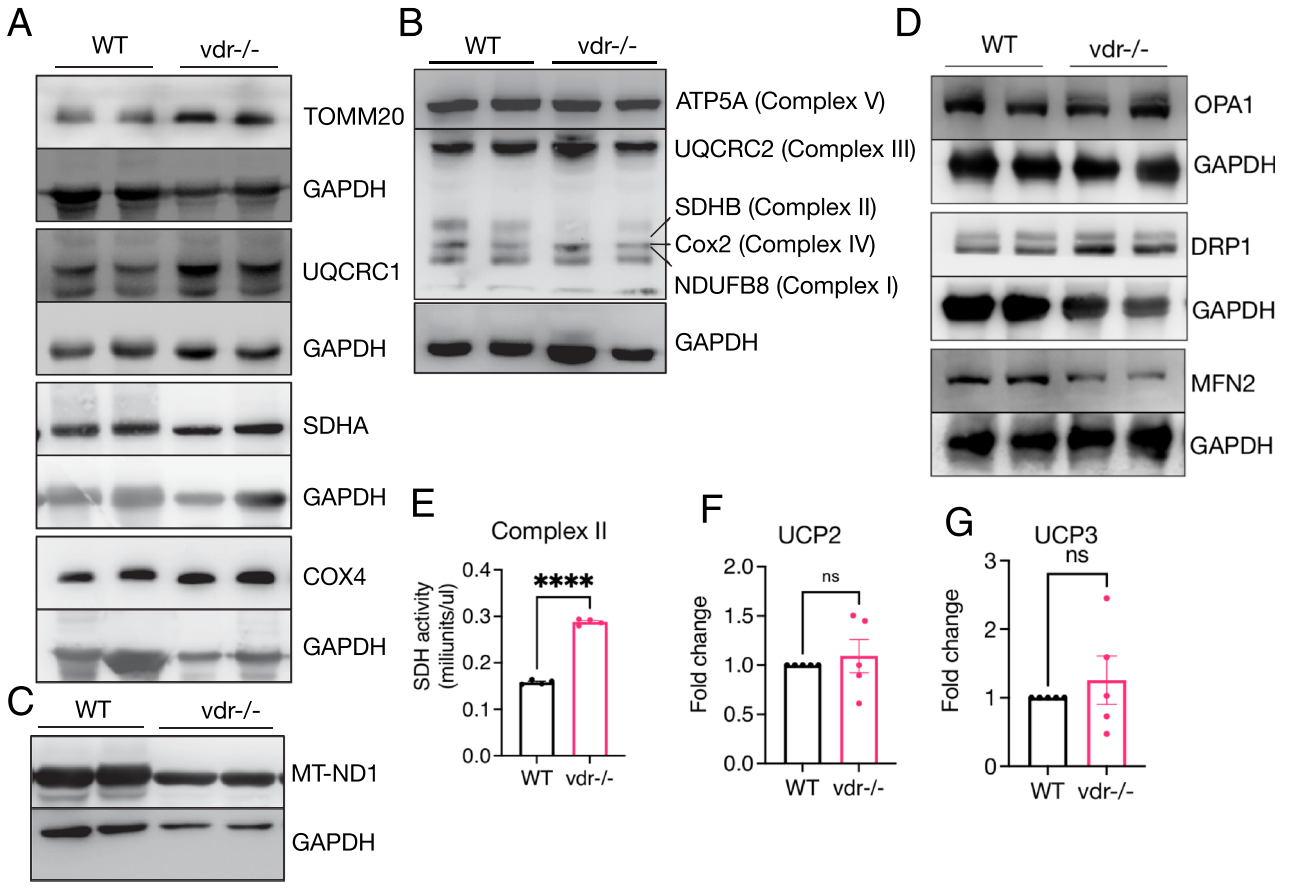

Figure 4 Energy insufficiency in vdr−/− skeletal muscles is not due to diminished mitochondrial activity. Representative western blots showing protein levels of *(A)* TOMM20, UQCRC1, SDHA, COX4, *(B)* OXPHOS complex components, *(C)* MT-ND1, and *(D)* OPA1, DRP1, and MFN2 in vdr−/− skeletal muscles. Quantification of western blots is shown in *Figure* S4. *(E)* SDH (complex II) activity in GAS muscles of WT and vdr−/− mice. *(F* and *G)* Real-time qRT–PCR quantitation of uncoupling proteins UCP2 *(F)* and UCP3 *(G)* in WT and vdr−/− mice. All graphs show mean ± SEM. Statistical significance was determined by unpaired *T*-test (*: $P < 0.05$, **: $P < 0.01$, ***: $P < 0.001$, ****: $P < 0.0001$).

DOI: 10.1002/jcsm.12841

muscles maintain mitochondrial mass comparable with that of WT. To have a better understanding about the functional capacity of the mitochondria in vdr−/− muscles, we checked the levels of different proteins involved in oxidative phosphorylation. UQCRC1, a member of the complex III of mitochondrial inner membrane, and SDHA, a subunit of complex II, did not show any statistically significant change in their protein levels (*Figures* 4A, S4b, and S4c). On the other hand, COX4, a complex IV subunit, was up-regulated in vdr−/− (*Figures* 4A and S4d). Western analysis using a combination of antibodies against different components of the ETC showed a decrease in the levels of SDHB in vdr−/− but not in subunits of other complexes (*Figure* 4B). Interestingly, reduced levels of SDHA, but not SDHB, are known to be associated with reduced OXPHOS.[33] Apart from the mitochondrial proteins imported from cytoplasm, the mitochondrial genome expresses 13 proteins that are essential functional components of all ETC and ATP synthase complexes.[34] We analysed the levels of MT-ND1, which is part of the complex I and found to be unchanged in vdr−/− muscles (*Figures* 4C and S4e).

Mitochondrial function is also modulated by fission and fusion of the mitochondria.[35] Western blot analyses of the fission protein Drp1 as well as the inner and outer membrane fusion proteins Opa1 and Mfn2 show that Mfn2 levels were slightly decreased in vdr−/− while others were unchanged, suggesting that there could be functional differences in the mitochondria of these mice (*Figure* 4D). To address this, we analysed the activity of respiratory complex II (SDH) in GAS muscles of these mice. Surprisingly, we found that the activity of SDH is significantly high in the vdr−/− mice, indicating increased mitochondrial activity (*Figure* 4E). Taken together, the data shown here suggest that although the vdr−/− skeletal muscles exhibit reduced ATP levels, it is not due to reduced mitochondrial activity. On the contrary, evidence suggests that these muscles may have increased mitochondrial activity. We did not find any significant differences in the levels of mitochondrial uncoupling proteins 2 and 3 (UCP2 and UCP3) in vdr−/− skeletal muscles, indicating that the discrepancy in mitochondrial activity and ATP levels is not due to the proton leakage induced by these proteins (*Figure* 4F and 4G). Interestingly, prolonged fasting, which leads to skeletal muscle wasting, is reported to result in increased mitochondrial activity in skeletal muscles.[36] This raises the likelihood that the observed defects could be due to deficiency in nutrient utilization rather than defective mitochondrial biogenesis or function.

vdr−/− mice exhibit defective glucose homeostasis

Skeletal muscle is the major site of glucose disposal in mammals, and insulin resistance in skeletal muscles accounts for 85–90% of glucose clearance impairment in type 2 diabetes.[37,38] The lack of insulin response in these mice in combination with reduced IR signalling in muscle suggests defective glucose clearance, which is expected to cause hyperglycaemia. But, on the contrary, fasting blood glucose levels of vdr−/− mice were significantly lower compared with WT at both 5 weeks (138.18 ± 5.02 mg/dL vs. 78.5 ± 7.69 mg/dL, P = 0.000003) and 7 weeks (95 ± 14.5 mg/dL vs. 148.6 ± 6.1 mg/dL, P = 0.0017) of age (*Figure* 5A and 5B). Random glucose levels at 7 weeks of age were also found to be lower in vdr−/− (*Figure* S5a).

A glucose tolerance test did not show any delay in glucose clearance in vdr−/− mice compared with WT at both 5 and 7 weeks of age (*Figure* 5C and 5D). The glucose levels remained low for vdr−/− even after glucose administration, but that is likely to be a reflection of lower baseline glucose levels. However, normalization of the values with respect to fasting glucose levels suggested that the kinetics of glucose uptake could be different in these mice (*Figure* S5b and S5c). Glut4 is the major glucose transporter in response to insulin, but during energy deprivation conditions, AMPK mediated up-regulation of Glut1 transporter accounts for increased glucose uptake independent of insulin.[39] qRT–PCR analysis revealed a 10-fold up-regulation of the Glut1 mRNA in the vdr−/− muscle (*Figure* 5E). Indeed, there was an up-regulation of glucose uptake by vdr−/− skeletal muscles as indicated by the higher accumulation of NBDG, a fluorescent analogue of glucose (*Figure* 5F). Taken together, these data show that there is indeed a systemic energy deprivation in vdr−/− mice, leading to hypoglycaemia, but glucose disposal in these mice are not dramatically affected. Serum lactate levels were also high in vdr−/− mice (7.42 ± 0.31 nmol/μL vs. 4.95 ± 0.44 nmol/μL, P = 0.0032), further confirming a systemic defect in energy metabolism in vdr −/− mice (*Figure* 5G).

The above-described observations suggested that these muscles use glucose at a higher rate through aerobic glycolysis. We found that vdr−/− muscles have higher levels of PDK4 (*Figure* 5H), which inhibits pyruvate dehydrogenase (PDH) complex to divert the pyruvate flux to aerobic glycolysis. But, PDH activity of vdr−/− muscles did not vary significantly in vdr−/− (6.91 ± 0.19 mU/mL for WT vs. 9.43 ± 2.52 mU/mL for vdr−/−; P = 0.23) (*Figure* 5I). Our previous results show increased activity of mitochondrial complexes in vdr−/−, indicating increased mitochondrial function (*Figure* 4E). Indeed, SDH staining of GAS muscle cryosections clearly shows increased SDH activity in the vdr−/− muscles (*Figure* 5J). The increased mitochondrial activity argues against oxidative-to-glycolytic metabolic shift in vdr−/− muscle fibres. Instead, we propose that the unchanged PDH and increased SDH activities indicate a compensatory mechanism in vdr−/− muscles to increase energy production, which is known to occur during energy deprivation conditions such as starvation.[36,40–42] The energy deprivation in these muscles despite having increased mitochondrial activity, glucose uptake, and normal levels of uncoupling pro-

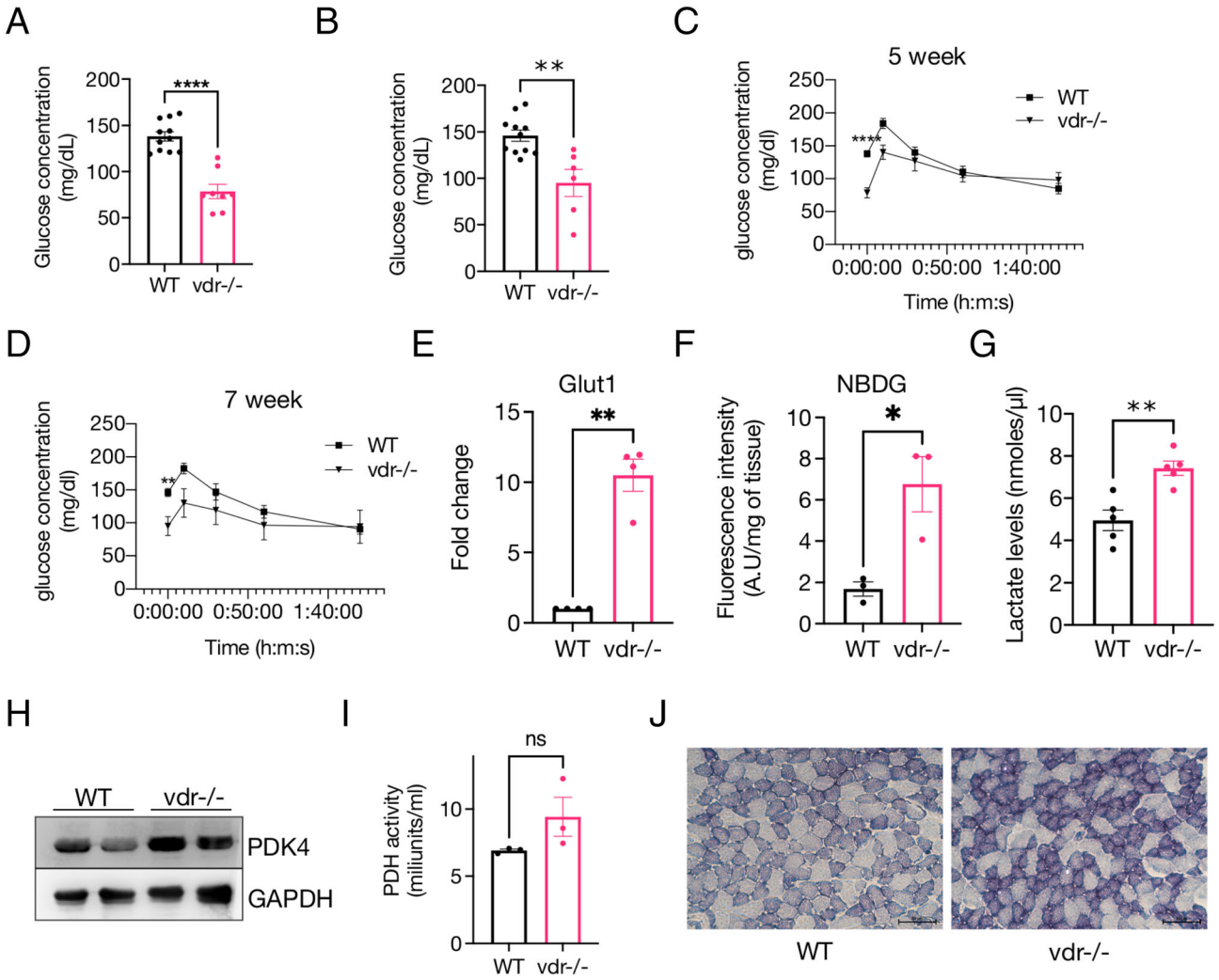

Figure 5 vdr−/− mice exhibit defective glucose homeostasis. *(A and B)* Fasting glucose levels of 5- *(A)* and 7-week-old *(B)* mice ($n \geq 6$). *(C and D)* Glucose tolerance test in 5- *(C)* and 7-week-old mice *(D)* ($n > 6$). *(E)* Hindlimb Glut1 mRNA levels quantified using qRT–PCR ($n = 4$). *(F)* Glucose uptake by GAS muscle as measured by the levels of fluorescence of NBDG in muscle ($n = 3$). *(G)* Serum lactate levels in WT and vdr−/− mice ($n = 5$). *(H)* Representative western blot showing the levels of PDK4 in WT and vdr−/− muscles. *(I)* PDH activity assay done on GAS muscles of vdr−/− and WT mice ($n = 3$). *(J)* Images of SDH stained WT and vdr−/− muscle sections. All graphs show mean ± SEM. Statistical significance was determined by unpaired *T*-test (*: $P < 0.05$, **: $P < 0.01$, ***: $P < 0.001$, ****: $P < 0.0001$).

teins suggested that these muscles may have a defect in mobilizing stored glucose.

Increased muscle glycogen accumulation is associated with defective glucose homeostasis in vdr−/− mice

Majority of glucose injected is disposed in skeletal muscles, and it is intriguing that despite normal glucose clearance, there is an energy deficit in vdr−/− skeletal muscles. So, we asked if there is any deficiency in utilization of glucose in these muscles. Glucose taken up by skeletal muscles is stored as glycogen. We checked whether the energy deprivation in skeletal muscles is associated with differences in glycogen levels. PAS staining of TA muscle sections revealed higher levels of glycogen in vdr−/− compared with WT (*Figure* 6A). To address whether this increase is associated with an increase in glycogen synthesis, we estimated glycogen synthase (GYS1) and phospho-GYS1 levels in the two groups and found a profound reduction in the inhibitory Ser641 phosphorylation of GYS1 (*Figure* 6B and 6C). Furthermore, consistent with reduced glycogen utilization, the activating Ser15 phosphorylation of glycogen phosphorylase (PYGM), an enzyme that degrades glycogen, was significantly reduced in vdr−/− (*Figure* 6D and 6E). Both the glycogen synthase and glycogen phosphorylase are regulated by calcium, and as expected, vdr−/− mice exhibit deficiency in serum calcium levels (*Figure* 6F). Moreover, the mRNA levels of glycogenin, an enzyme required to initiate glycogen bio-

DOI: 10.1002/jcsm.12841

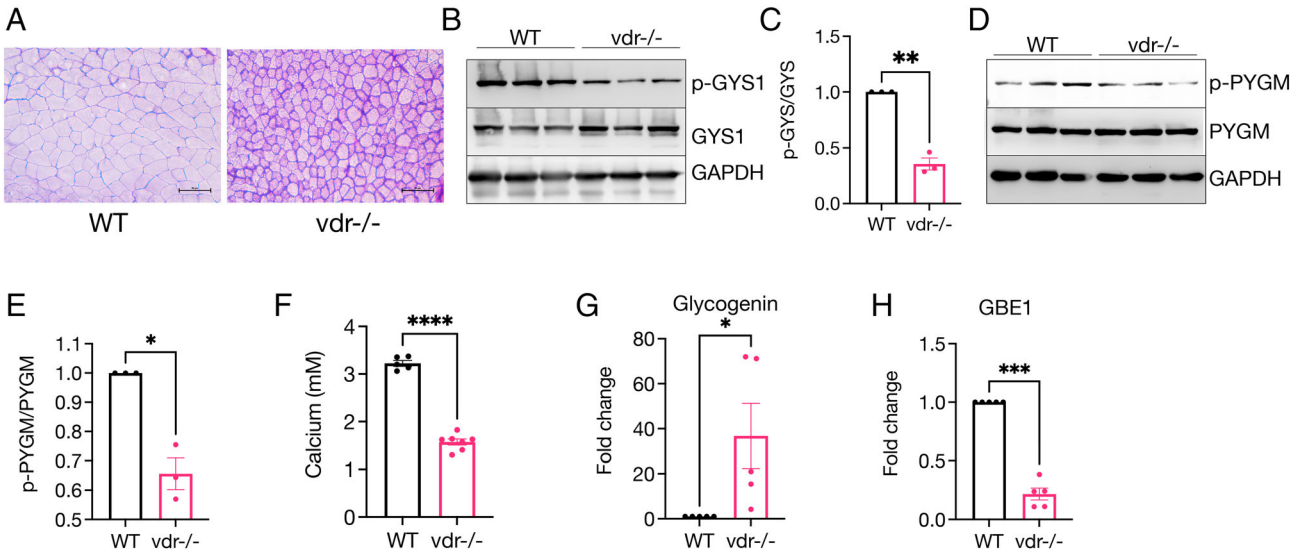

Figure 6 Dysregulation of glycogen synthase and phosphorylase activities lead to increased glycogen accumulation in vdr−/− skeletal muscles. *(A)* Micrographs of PAS stained transverse sections of GAS muscles from WT and vdr−/− mice. *(B and C)* Western blot *(B)* and densitometric quantitation *(C)* for GYS1 (n = 3). *(D and E)* Western blot *(D)* and densitometric quantitation *(E)* of PYGM (n = 3). *(F)* Serum calcium levels in WT and vdr−/− mice (n = 4). *(G and H)* qRT–PCR quantitation of glycogenin *(G)* and GBE1 *(H)* mRNAs in TA muscles (n = 5). All graphs show mean ± SEM. Statistical significance was determined by unpaired *T*-test (*: $P < 0.05$, **: $P < 0.01$, ***: $P < 0.001$, ****: $P < 0.0001$).

synthesis, were up-regulated in vdr−/− muscles (*Figure* 6G), supporting increased glycogen synthesis. Interestingly, we also found that the mRNA levels of glycogen branching enzyme (GBE1), whose depletion leads to accumulation of abnormal glycogen, were down-regulated (*Figure* 6H). Taken together, these results suggest that skeletal muscles of vdr−/− mice exhibit a carbohydrate utilization defect characterized by increased glycogen accumulation. Skeletal muscle glycogen storage disorders are known to induce systemic and skeletal muscle energy imbalance and trigger atrophy.[43]

Discussion

Several factors are known to lead to skeletal muscle atrophy, ranging from inactivity and starvation to genetic disorders and other diseases such as diabetes, cancer, and tuberculosis.[10,21] Although the vdr−/− mice are known to exhibit severe skeletal muscle atrophy,[1] and vitamin D-deficient individuals exhibit varying degrees of myopathies,[44] the underlying mechanisms are not well understood. Because these mice exhibit a growth defect as well, it is likely that the reduced muscle mass could be a manifestation of reduced growth than muscle wasting. But our results as well as others have shown that skeletal muscles of these mice exhibit increased expression of atrophy markers such as MurF1, Fbxo32, and the Foxo1 transcription factor.[15,45] Moreover, our data show that the muscle proteostasis defect is not observed in 3-week-old mice. Increased muscle protein degradation has been reported in vitamin D-deficient rat models as well.[12] Further granularity of proteostasis defects was achieved by identifying that the decrease in protein synthesis is limited to the fasting state in vdr−/− mice while absorptive state protein synthesis was not affected. We propose that the availability of nutrients in the postprandial state is responsible for maintaining normal protein synthesis rates while energy deprivation associated with impaired glycogen utilization is responsible for decreased protein synthesis during the fasting state in vdr−/− skeletal muscles.

Based on the evidence presented here, we propose the following model for the development of skeletal muscle atrophy in vdr−/− mice (*Figure* 7). The abnormal accumulation of glycogen in vdr−/− muscles, driven by increased glycogen synthase activity and decreased glycogen phosphorylase activity, renders it unavailable for energy production during the post-absorptive state leading to a state of constitutive energy deprivation and to the activation of the AMPK pathway. High AMPK activity in turn leads to higher glucose uptake by muscle with the aid of increased Glut1 expression,[39] and its chronic activation contributes to increased glycogen accumulation in skeletal muscles.[46] This feed forward loop of glucose uptake and glycogen synthesis with a reduction in the glycogen phosphorylase activity could elevate glucose consumption by vdr−/− muscles and subsequent systemic glucose depletion especially during post-absorptive state. The increased serum lactate levels, which could be the result of the body's attempt to increase the liver gluconeogenesis in vdr−/− mice, support this hypothesis. The increased muscle proteolysis observed in vdr−/− could also function to ensure supply of other gluconeogenesis substrates such as alanine.

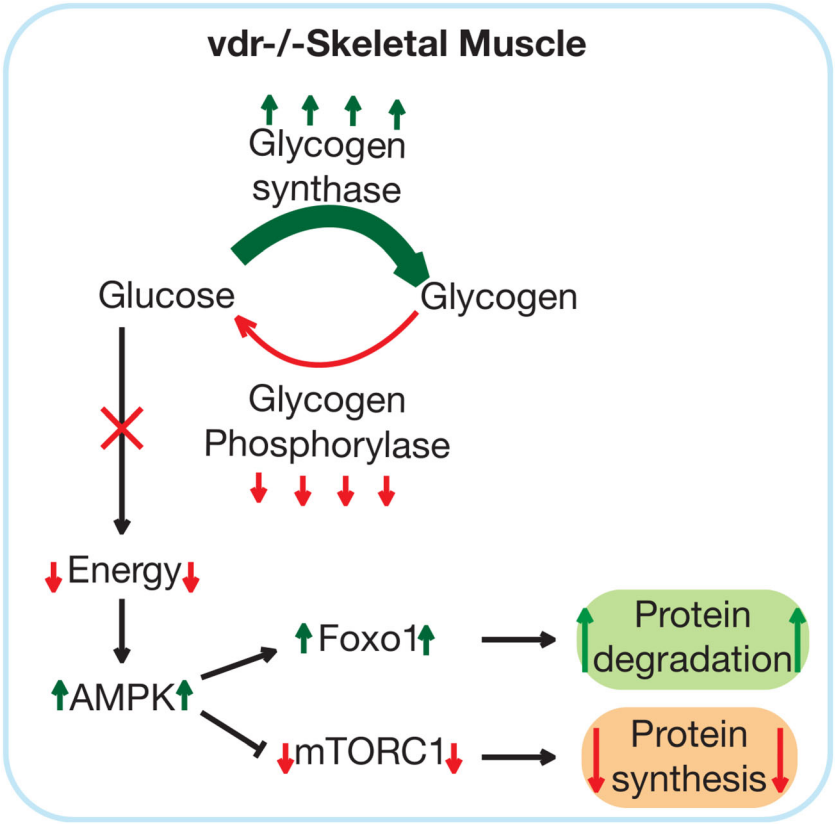

Figure 7 Glycogen storage disorder leads to skeletal muscle atrophy in vdr−/− mice. Dysregulation of glycogen synthase and phosphorylase in the absence of VDR signalling leads to increased glycogen accumulation in skeletal muscles and subsequent energy deprivation and glucose homeostasis defects. These defects lead to increased protein degradation and decreased protein synthesis, causing skeletal muscle atrophy.

However, this seems insufficient in maintaining fasting glucose levels in vdr−/− mice. The defects in liver metabolism require to be studied further to resolve this issue. The increase in the mitochondrial activity observed in the muscles of these mice indicates that the energy deficiency is not driven by mitochondrial damage. The increased mitochondrial activity may reflect the attempt by the muscles to counterbalance the energy insufficiency. These data clearly suggest that the energy deprivation induced by the glycogen storage defect is causative for the muscle wasting in vdr−/− mice.

This model could be applicable to humans as well. Interestingly, skeletal muscles of athletes with severe vitamin D-deficient have been reported to show increased glycogen granules.[44] Moreover, the susceptibility of individuals with vitamin D deficiency to develop insulin resistance is also well documented, showing the relationship between vitamin D signalling and glucose homeostasis.[47] Other glycogen storage diseases, particularly those involving mutations in the glycogen branching enzyme GBE1, where stored glycogen cannot be utilized, display skeletal muscle atrophy and hypoglycaemia.[48,49] Further studies are underway to delineate the mechanisms by which the lack of vitamin D signalling leads to dysregulation of glycogen synthase, glycogen phosphorylase, and glycogen storage disorder. Because calcium is a well-known activator of glycogenolysis and repressor of glycogen synthesis, it is possible that the lower calcium availability could be one of the reasons for the abnormal glycogen accumulation in vdr−/− skeletal muscles. Absence of such drastic metabolic defects in high calcium supplemented vdr−/− mice support this hypothesis.[1,16]

Conclusions

Data presented here show that there is a proteostasis defect in vdr−/− skeletal muscles that is characterized by increased protein degradation and decreased fasting protein synthesis. These muscles also exhibit constitutive down-regulation of mTORC1 pathway. Further analysis suggested that the mTORC1 pathway defect as well as the proteostasis defects could be driven by abnormal activation of AMPK pathway in these skeletal muscles. Systemic as well as skeletal muscle energy deprivation caused by a glycogen storage defect accounts for the AMPK pathway and thereby proteostasis defects and atrophy. Taken together, our experiments reveal defective energy metabolism that is characterized by increased glycogen storage in vdr−/− skeletal muscle as the root cause of severe atrophy.

Acknowledgements

We are grateful to Mr. Khem Singh Negi for genotyping mice and other technical help, and to Mr. B. N. Roy for help with histopathology experiments. The authors of this manuscript certify that they comply with the ethical guidelines for authorship and publishing in the *Journal of Cachexia, Sarcopenia and Muscle*.[50]

Conflict of interest

The authors declare there is no conflict of interest.

Funding

The authors thank DBT, Government of India (BT/PR29599/PFN/20/1393/2018 for G.A.A. and S.D.G., BT/PR27638/GET/119/266/2018 for G.A.A.) and DST-SERB, Government of India (Ramanujan Fellowship—SB/S21RJN-063/2016 and early career award—ECR/2017/000115) for research grants.

Online supplementary material

Additional supporting information may be found online in the Supporting Information section at the end of the article.

Figure S1. vdr−/− skeletal muscles exhibit defective proteostasis. a) Body weight (in grams) of WT and vdr−/− mice at 3, 5 and 7 weeks of age ($n > 5$). b-d) TA, GAS and QUAD muscle weight of 7-week-old WT and vdr−/− (n > 5). e&f) H&E stained transverse sections of TA (e) and GAS (f) muscles. g) Cross sectional areas of muscle fibers in WT, vdr−/− mice. Percentage of fibers that have cross section areas less than 100μm^2, 100-300 μm^2, 300-500 μm^2 and more than 500μm^2 are plotted. Areas were calculated using image J software. All graphs show mean±SEM. Statistical significance was determined by unpaired T-test (*: $p < 0.05$, **: $p < 0.01$, ***: $p < 0.001$, ****: $p < 0.0001$).

Figure S2. Foxo3 is unaffected in vdr−/− muscles. a) Representative western blot showing the total protein levels of FOXO3 in 3-week and 7-week-old skeletal muscles. b&c) Western blot showing nucleo-cytoplasmic distribution of FOXO3 at 3 weeks (b) and 7 weeks (c) of age. No nuclear localization is seen. Anti-TBP antibody was used as nuclear loading control.

Figure S3. vdr−/− liver exhibit reduced mTORC1 activity. a&b) Western blots showing the levels of phsopho-S6 (a) and phospho-AMPK (b) in the liver of 7-week-old mice. c) Western blot using anti-puromycin antibody for estimation of fasting protein synthesis in the liver of 7-week-old WT and vdr−/−.

Figure S4. Mitochondrial mass is unaffected in vdr−/− skeletal muscles. Densitometric quantitation of a) TOMM20 ($n = 6$), b) UQCRC1 ($n = 3$), c) SDHA (n = 3), d) COX4 ($n = 4$), and e) MT-ND1 (n = 3). Representative blots are shown in Figure 4. All graphs show mean±SEM. Statistical significance was determined by unpaired T-test (*: $p < 0.05$, **: $p < 0.01$, ***: $p < 0.001$, ****: $p < 0.0001$).

Figure S5. vdr−/− mice exhibit defective glucose homeostasis. a) Random glucose levels of 7-week-old WT and vdr−/− ($n > 4$). b&c) Blood glucose levels at different time points after intraperitoneal injection of glucose in 5-week-old (b) and 7-week-old (c) mice. Values are normalised with fasting glucose levels (time 0). Normalization was done by dividing the glucose concentrations different time points with that of time 0. Unnormalized values are plotted in Figure 4d & e. All graphs show mean±SEM. Statistical significance was determined by unpaired T-test (*: $p < 0.05$, **: $p < 0.01$, ***: $p < 0.001$, ****: $p < 0.0001$).

References

1. Endo I, Inoue D, Mitsui T, Umaki Y, Akaike M, Yoshizawa T, et al. Deletion of vitamin D receptor gene in mice results in abnormal skeletal muscle development with deregulated expression of myoregulatory transcription factors. *Endocrinology* 2003; **144**:5138–5144.
2. Montenegro KR, Cruzat V, Carlessi R, Newsholme P. Mechanisms of vitamin D action in skeletal muscle. *Nutr Res Rev* 2019;**32**:192–204.
3. Bischoff-Ferrari HA, Borchers M, Gudat F, Dürmüller U, Stähelin HB, Dick W. Vitamin D receptor expression in human muscle tissue decreases with age. *J Bone Miner Res* 2004;**19**:265–269.
4. Girgis CM, Mokbel N, Cha KM, Houweling PJ, Abboud M, Fraser DR, et al. The vitamin D receptor (VDR) is expressed in skeletal muscle of male mice and modulates 25-hydroxyvitamin D (25OHD) uptake in myofibers. *Endocrinology* 2014;**155**: 3227–3237.
5. Rennie MJ, Wackerhage H, Spangenburg EE, Booth FW. Control of the size of the human muscle mass. *Annu Rev Physiol* 2004;**66**:799–828.
6. James HA, O'Neill BT, Nair KS. Insulin regulation of proteostasis and clinical implications. *Cell Metab* 2017;**26**:310–323.
7. Argilés JM, Campos N, Lopez-Pedrosa JM, Rueda R, Rodriguez-Mañas L. Skeletal muscle regulates metabolism via interorgan crosstalk: roles in health and disease. *J Am Med Dir Assoc* 2016;**17**:789–796.
8. Wolfe RR. The underappreciated role of muscle in health and disease. *Am J Clin Nutr* 2006;**84**:475–482.

9. Sharma A, Oonthonpan L, Sheldon RD, Rauckhorst AJ, Zhu Z, Tompkins SC, et al. Impaired skeletal muscle mitochondrial pyruvate uptake rewires glucose metabolism to drive whole-body leanness. *Elife* 2019;**8**.
10. Fanzani A, Conraads VM, Penna F, Martinet W. Molecular and cellular mechanisms of skeletal muscle atrophy: an update. *J Cachexia Sarcopenia Muscle* 2012;**3**: 163–179.
11. Bonaldo P, Sandri M. Cellular and molecular mechanisms of muscle atrophy. *Dis Model Mech* 2013;**6**:25–39.
12. Bhat M, Kalam R, Qadri SS, Madabushi S, Ismail A. Vitamin D deficiency-induced muscle wasting occurs through the ubiquitin proteasome pathway and is partially corrected by calcium in male rats. *Endocrinology* 2013;**154**:4018–4029.
13. Gogulothu R, Nagar D, Gopalakrishnan S, Garlapati VR, Kallamadi PR, Ismail A. Disrupted expression of genes essential for skeletal muscle fibre integrity and energy metabolism in Vitamin D deficient rats. *J Steroid Biochem Mol Biol* 2020;**197**: 105525.
14. Girgis CM, Cha KM, So B, Tsang M, Chen J, Houweling PJ, et al. Mice with myocyte deletion of vitamin D receptor have sarcopenia and impaired muscle function. *J Cachexia Sarcopenia Muscle* 2019;**10**: 1228–1240.
15. Chen S, Villalta SA, Agrawal DK. FOXO1 mediates Vitamin D deficiency-induced insulin resistance in skeletal muscle. *J Bone Miner Res* 2016;**31**:585–595.
16. Li YC, Pirro AE, Amling M, Delling G, Baron R, Bronson R, et al. Targeted ablation of the vitamin D receptor: an animal model of vitamin D-dependent rickets type II with alopecia. *Proc Natl Acad Sci U S A* 1997;**94**:9831–9835.
17. Yoshizawa T, Handa Y, Uematsu Y, Takeda S, Sekine K, Yoshihara Y, et al. Mice lacking the vitamin D receptor exhibit impaired bone formation, uterine hypoplasia and growth retardation after weaning. *Nat Genet* 1997;**16**:391–396.
18. O'Neill BT, Lee KY, Klaus K, Softic S, Krumpoch MT, Fentz J, et al. Insulin and IGF-1 receptors regulate FoxO-mediated signaling in muscle proteostasis. *J Clin Invest* 2016;**126**:3433–3446.
19. Kwan AYM, Hartman ML. IGF-I measurements in the diagnosis of adult growth hormone deficiency. *Pituitary* 2007;**10**: 151–157.
20. Lecker SH, Jagoe RT, Gilbert A, Gomes M, Baracos V, Bailey J, et al. Multiple types of skeletal muscle atrophy involve a common program of changes in gene expression. *FASEB J* 2004;**18**:39–51.
21. Russell AP. Molecular regulation of skeletal muscle mass. *Clin Exp Pharmacol Physiol* 2010;**37**:378–384.
22. Sandri M, Sandri C, Gilbert A, Skurk C, Calabria E, Picard A, et al. Foxo transcription factors induce the atrophy-related ubiquitin ligase atrogin-1 and cause skeletal muscle atrophy. *Cell* 2004;**117**:399–412.
23. Paddon-Jones D, Sheffield-Moore M, Cree MG, Hewlings SJ, Aarsland A, Wolfe RR, et al. Atrophy and impaired muscle protein synthesis during prolonged inactivity and stress. *J Clin Endocrinol Metab* 2006;**91**: 4836–4841.
24. Sonenberg N, Hinnebusch AG. Regulation of translation initiation in eukaryotes: mechanisms and biological targets. *Cell* 2009;**136**:731–745.
25. Thoreen CC, Chantranupong L, Keys HR, Wang T, Gray NS, Sabatini DM. A unifying model for mTORC1-mediated regulation of mRNA translation. *Nature* 2012;**485**: 109–113.
26. Kamei Y, Mizukami J, Miura S, Suzuki M, Takahashi N, Kawada T, et al. A forkhead transcription factor FKHR up-regulates lipoprotein lipase expression in skeletal muscle. *FEBS Lett* 2003;**536**:232–236.
27. Zeitz U, Weber K, Soegiarto DW, Wolf E, Balling R, Erben RG. Impaired insulin secretory capacity in mice lacking a functional vitamin D receptor. *FASEB J* 2003;**17**: 509–511.
28. Chibalin AV, Yu M, Ryder JW, Song XM, Galuska D, Krook A, et al. Exercise-induced changes in expression and activity of proteins involved in insulin signal transduction in skeletal muscle: differential effects on insulin-receptor substrates 1 and 2. *Proc Natl Acad Sci U S A* 2000;**97**:38–43.
29. Inoki K, Zhu T, Guan K-L. TSC2 mediates cellular energy response to control cell growth and survival. *Cell* 2003;**115**: 577–590.
30. Brugarolas J, Lei K, Hurley RL, Manning BD, Reiling JH, Hafen E, et al. Regulation of mTOR function in response to hypoxia by REDD1 and the TSC1/TSC2 tumor suppressor complex. *Genes Dev* 2004;**18**: 2893–2904.
31. Reznick RM, Shulman GI. The role of AMP-activated protein kinase in mitochondrial biogenesis. *J Physiol* 2006;**574**:33–39.
32. Whitaker-Menezes D, Martinez-Outschoorn UE, Flomenberg N, Birbe RC, Witkiewicz AK, Howell A, et al. Hyperactivation of oxidative mitochondrial metabolism in epithelial cancer cells in situ: visualizing the therapeutic effects of metformin in tumor tissue. *Cell Cycle* 2011;**10**:4047–4064.
33. Guzy RD, Sharma B, Bell E, Chandel NS, Schumacker PT. Loss of the SdhB, but Not the SdhA, subunit of complex II triggers reactive oxygen species-dependent hypoxia-inducible factor activation and tumorigenesis. *Mol Cell Biol* 2008;**28**:718–731.
34. Ott M, Amunts A, Brown A. Organization and regulation of mitochondrial protein synthesis. *Annu Rev Biochem* 2016;**85**: 77–101.
35. Youle RJ, van der Bliek AM. Mitochondrial fission, fusion, and stress. *Science* 2012; **337**:1062–1065.
36. Bourguignon A, Rameau A, Toullec G, Romestaing C, Roussel D. Increased mitochondrial energy efficiency in skeletal muscle after long-term fasting: its relevance to animal performance. *J Exp Biol* 2017;**220**: 2445–2451.
37. DeFronzo RA, Gunnarsson R, Björkman O, Olsson M, Wahren J. Effects of insulin on peripheral and splanchnic glucose metabolism in noninsulin-dependent (type II) diabetes mellitus. *J Clin Invest* 1985;**76**:149–155.
38. Defronzo RA. Banting Lecture. From the triumvirate to the ominous octet: a new paradigm for the treatment of type 2 diabetes mellitus. *Diabetes* 2009;**58**:773–795.
39. Jing M, Cheruvu VK, Ismail-Beigi F. Stimulation of glucose transport in response to activation of distinct AMPK signaling pathways. *Am J Physiol Cell Physiol* 2008; **295**:C1071–C1082.
40. Tsintzas K, Jewell K, Kamran M, Laithwaite D, Boonsong T, Littlewood J, et al. Differential regulation of metabolic genes in skeletal muscle during starvation and refeeding in humans. *J Physiol* 2006;**575**:291–303.
41. Wu P, Blair PV, Sato J, Jaskiewicz J, Popov KM, Harris RA. Starvation increases the amount of pyruvate dehydrogenase kinase in several mammalian tissues. *Arch Biochem Biophys* 2000;**381**:1–7.
42. Furuyama T, Kitayama K, Yamashita H, Mori N. Forkhead transcription factor FOXO1 (FKHR)-dependent induction of PDK4 gene expression in skeletal muscle during energy deprivation. *Biochem J* 2003;**375**: 365–371.
43. Marion RW, Paljevic E. The glycogen storage disorders. *Pediatr Rev* 2020;**41**:41–44.
44. Polly P, Tan TC. The role of vitamin D in skeletal and cardiac muscle function. *Front Physiol* 2014;**5**:145.
45. Gopinath SD. Inhibition of Stat3 signaling ameliorates atrophy of the soleus muscles in mice lacking the vitamin D receptor. *Skelet Muscle* 2017;**7**:2.
46. Hunter RW, Treebak JT, Wojtaszewski JFP, Sakamoto K. Molecular mechanism by which AMP-activated protein kinase activation promotes glycogen accumulation in muscle. *Diabetes* 2011;**60**:766–774.
47. dos Santos LR, Lima AGA, Braz AF, de Sousa Melo SR, Morais JBS, Severo JS, et al. Role of vitamin D in insulin resistance in obese individuals. *Forum Nutr* 2017;**42**:1–6.
48. Iijima H, Iwano R, Tanaka Y, Muroya K, Fukuda T, Sugie H, et al. Analysis of GBE1 mutations via protein expression studies in glycogen storage disease type IV: a report on a non-progressive form with a literature review. *Mol Genet Metab Rep* 2018;**17**:31–37.
49. Fyfe JC, Kurzhals RL, Hawkins MG, Wang P, Yuhki N, Giger U, et al. A complex rearrangement in GBE1 causes both perinatal hypoglycemic collapse and late-juvenile-onset neuromuscular degeneration in glycogen storage disease type IV of Norwegian forest cats. *Mol Genet Metab* 2007;**90**:383–392.
50. von Haehling S, Morley JE, Coats AJS, Anker SD. Ethical guidelines for publishing in the *Journal of Cachexia, Sarcopenia and Muscle*: update 2019. *J Cachexia Sarcopenia Muscle* 2019;**10**:1143–1145.